Systems & Control Transactions

Original Research Article
Peer Reviewed Conference Proceeding
ESCAPE 36 - European Symposium on Computer Aided Process Engineering
Sheffield, UK. 21-24 June 2026

PSE PRESS

A General Framework for Model Recognition in Chemical Reactor Systems Using Artificial Neural Networks Classifiers

Emmanuel Agunloye, Asterios Gavriilidis, and Federico Galvanin*

Department of Chemical Engineering, University College London, London WC1E 7JE, UK
*Corresponding Author: f.galvanin@ucl.ac.uk

ABSTRACT

The identification of predictive mathematical model structures (i.e. set of model equations) is essential for the development of digital twin models of chemical reactor systems. Recent work demonstrated the use of artificial neural networks (ANNs) for kinetic model recognition in a conceptual batch reaction experimental system. In practical chemical processes, however, system behaviour is governed not only by reaction kinetics but also by reactor hydrodynamics and system thermodynamics. While a very recent study incorporated hydrodynamic effects, this work integrates the three aspects: reaction kinetics, reactor hydrodynamics, and system thermodynamics, to develop a general reactor modelling recognition framework. The framework, which comprises three modules: 1) model generator module; 2) data generation module; and 3) ANN classifier module, was applied to a case study of benzoic acid esterification in a Taylor vortex flow reactor system. Analysing the framework's sensitivity, results showed that ANN performance in classification deteriorates under increasing measurement noise but can be improved by increasing the number of simulated experiments. Further results show that extensive hyperparameter optimisation of ANN architectures provides no benefit over a fixed ANN architecture. This study highlights the potential of ANN-based frameworks for reactor model recognition while underscoring the dominant role of experimental design and data quality over network hyperparameter tuning.

Keywords: Modelling, Machine Learning, Optimization, Modelling and Simulations, Process Operations, Hybrid modelling, Artificial neural networks, Taylor vortex flow reactor

1.0 INTRODUCTION

Digital twin (DT) technology is transforming the way chemical and pharmaceutical processes are designed, monitored, and optimised [1 - 3]. A digital twin combines real-time data from a physical process with predictive computational models to enable autonomous operation and closed-loop optimisation [2]. In pharmaceutical manufacturing, DTs play a central role in accelerating process development, ensuring consistent product quality, and supporting regulatory compliance.

Despite the rapid rise of data-driven and machine learning (ML)-based digital twins, their adoption in safety-critical industries such as pharmaceuticals has been hindered by concerns about reliability, interpretability, and robustness [4]. Purely data-driven models can capture system trends efficiently but often fail to extrapolate beyond the training domain, leading to unsafe or suboptimal operation when process conditions change. To overcome these limitations, hybrid digital twins—which combine the computational efficiency of ML with the physical interpretability of first-principles models—have gained increasing attention [5-7].

Within this context, model identification remains a crucial step. Reliable digital twins require high-fidelity process models capable of representing reaction kinetics, reactor hydrodynamics, and thermodynamic interactions [8]. Recent research has demonstrated the use of artificial neural networks (ANNs) for rapid kinetic model recognition and optimal experimental design, particularly in batch reactor systems [9, 10]. However, these studies often neglected hydrodynamic and thermal effects whose representation is critical in nonisothermal flow reactors, which are increasingly central to pharmaceutical

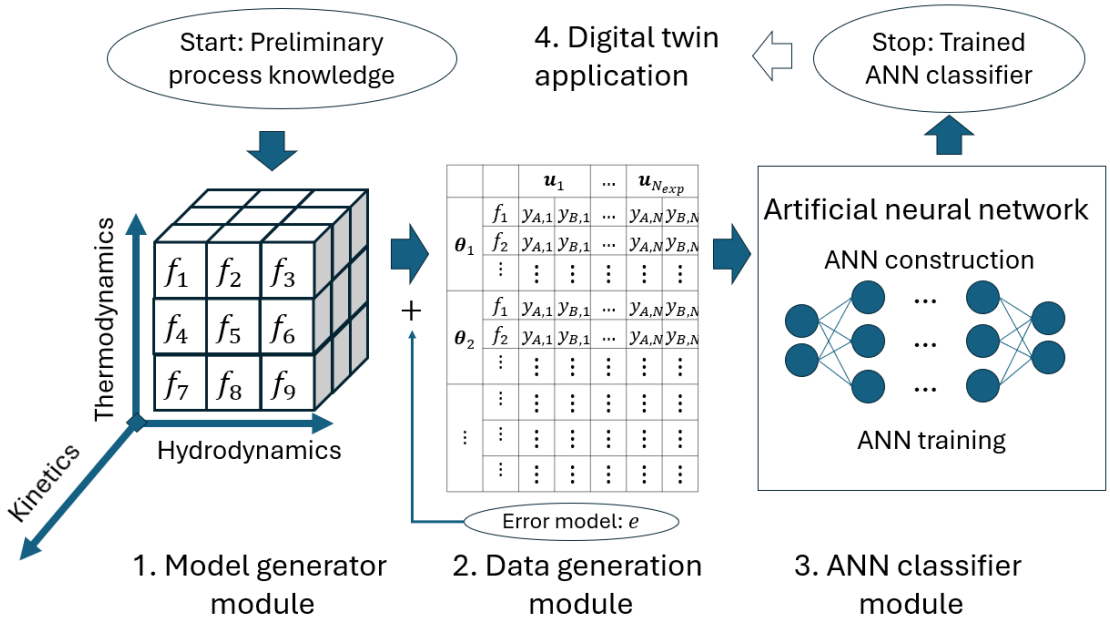

Figure 1: ANN hybrid modelling framework with 3-dimensional physics-based model generator

scale-up.

The present work extends previous ANN-based frameworks [9–11] by incorporating hydrodynamics and thermodynamics explicitly into the model recognition process. The extended framework is subsequently evaluated with respect to data quality and ANN architectural complexity to assess its scientific robustness and computational efficiency. The proposed framework identifies the most suitable reactor model structure among a library of possible configurations including kinetics, hydrodynamics, and energy interactions. This hybrid approach enables fast yet physically grounded model recognition — a key requirement for reliable DT implementation.

2.0 METHODOLOGY

The proposed hybrid framework comprises three interconnected modules (Fig. 1): 1. Model Generator Module, 2. Data Generation Module, and 3. ANN Classifier Module, for subsequent application as a digital twin.

2.1 Model Generator Module

The model generator defines the library of possible reactor models, organised as a three-dimensional tensor. Each axis of this tensor corresponds to a distinct modelling domain:

- Reaction Kinetics: Alternative rate-law formulations capturing alternative mechanistic hypotheses;
- Reactor Hydrodynamics: Different reactor flow models, considering in this work continuously stirred tank reactor (CSTR) and plug flow reactor (PFR) representations;
- System Thermodynamics: Alternative energy balance assumptions—adiabatic and isothermal operations.

Each model structure i is generally described by a system of differential and algebraic equations that can be written as:

$$\boldsymbol{f}_i(\boldsymbol{x}, \dot{\boldsymbol{x}}, \boldsymbol{u}, \theta, \tau) = \boldsymbol{0}$$
$$\boldsymbol{y} = \boldsymbol{g}(\boldsymbol{x}) \quad (1)$$

where $\boldsymbol{x} \in \mathcal{X} \subseteq \mathbb{R}^{n_x}$: vector of state variables (e.g., concentrations and temperatures), $\dot{\boldsymbol{x}} \in \dot{\mathcal{X}} \subseteq \mathbb{R}^{n_x}$: vector of time derivatives of the state variables; $\boldsymbol{u} \in \mathcal{U} \subseteq \mathbb{R}^{n_u}$: vector of control/input variables (e.g., inlet temperature, stream flow rates and composition in flow reaction systems); $\theta \in \boldsymbol{\Theta} \subseteq \mathbb{R}^{n_\theta}$: vector of model parameters (e.g., reaction Arrhenius parameters); τ: space time variable; $\boldsymbol{y} \in \boldsymbol{\mathcal{Y}} \subseteq \mathbb{R}^{n_y}$: vector of measured variables.

2.2 Data Generation Module

The data generation module produces synthetic datasets by simulating each model structure over the defined parameter and design spaces, following three main features:

- Parameter Space Sampling: Kinetic parameter sets $\{\dots, \theta_i, \dots\}$ are sampled from the feasible space of model parameters [9] using Latin hypercube

sampling (LHS) to ensure space-filling coverage.

- Experimental Design Space Sampling: Operating conditions $\boldsymbol{u}_i = [\boldsymbol{c}_0, T, \tau]$, denoting feed concentrations, temperature, and residence time, respectively are randomly designed using the Latin hypercube sampling technique from the experimental design space $\boldsymbol{\varphi}$ before employing the models to simulate the experimental conditions.
- Noise Modelling: to assess the impact of data quality on model identification Gaussian noise (e) with zero mean and relative variance ω has been varied between 0.01 and 0.1, and added to model outputs $\hat{\boldsymbol{y}}$ to mimic measurement uncertainty in real experiments, i.e.,

$$e = \mathcal{N}[0, \sigma^2 = (\omega y)^2] \quad (2)$$

The simulated data comprise model outputs and their labels, which serve as training and validation data set for ANN classifiers.

2.3 ANN Classifier Module

The third module performs model recognition using ANNs trained to classify which model structure best represents the test data. Two ANN architectures are considered:

- ANNfix: Fixed network structure comprising 3 hidden layers with 160 nodes per layer
- ANNopt: Hyperparameter-optimised network, varying the number of hidden layers (n_h = 1 – 5) and the number of nodes per layer (n = 32-256)

The ANN classification transformation can be described as:

$$p_i = \phi_{N_L}(\dots \phi_1(\boldsymbol{w}^T \boldsymbol{y} + \boldsymbol{b}) \dots); \forall i = [1, 2, \dots, N_m] \quad (3)$$

where p_i is the probability of ANN selection calculated for Model f_i; $\boldsymbol{w}$ and $\boldsymbol{b}$ are the weights and biases in ANN nodes respectively; ϕ_1 is the activation function of layer 1. For classification, SoftMax activation function is used in Layer N_L while ReLU activation function is used in all the preceding layers [12]. ANN parameters $\boldsymbol{w}$ and $\boldsymbol{b}$ are estimated from model training using standard backpropagation with categorical cross-entropy as the objective function. Classification accuracy $\mathrm{Acc}_{\Psi_{\text{test}}}$—the proportion of correctly identified model structures in the test dataset, expressed in Eq. (4)—serves as the primary performance metric.

$$\mathrm{Acc}_{\Psi_{\text{test}}} = \frac{N_{\Psi_{\text{test}} \wedge \hat{l}_i = l_i}}{N_{\Psi_{\text{test}}}} \cdot 100\% \quad (4)$$

where $N_{\Psi_{\text{test}}}$ is the number of samples in the test dataset; $N_{\Psi_{\text{test}} \wedge \hat{l}_i = l_i}$ is the number of test samples where the model label has been correctly classified.

3.0 CASE STUDY

The synthesis case study considered in this work is related to benzoic acid esterification [13] in a Taylor vortex reactor (TVR). In this esterification reaction, benzoic acid (BA) reacts with ethanol (EtOH) to produce water (W) and ethylbenzoate (EB) in a single reaction shown in Eq. 5. This reaction can be described using two rival reaction kinetics shown in equations M1 and M2, providing two options along the kinetic submodel dimension [13]

$$BA + EtOH \rightarrow W + EB \quad (5)$$

$$k_1 c_{BA} c_{EtOH} \quad (M1)$$

$$\frac{k_1 c_{BA} c_{EtOH}}{(1 + K_W c_W)^2} \quad (M2)$$

where: $k_1 = \exp\left(-KP_1 - \frac{KP_2 \times 10000}{RT}\left[\frac{1}{T} - \frac{1}{T_{ref}}\right]\right)$;

$$T_{ref} = 378.15\ K \quad (6)$$

Thus, $\boldsymbol{u} = [c_{BA}(0), T, F_{total}]$; $\hat{\boldsymbol{y}} = [c_{BA}, c_{EtOH}, c_W, c_{EB}, T]$ and $\theta = [KP_1, KP_2, K_W]$.

A TVR of 10 mL volume with 9.5 and 10.2 mm in annulus inner and outer diameters is employed. Because of its rotating concentric cylinders (inner rotor and outer stator as shown in Fig. 2), the TVR offers mixing conditions that can vary from continuously stirred tank reactor (CSTR) (Eq. R1) to plug flow reactor (PFR) (Eq. R2) [14], so that a trained ANN within the hybrid framework will be able to recognise the prevailing hydrodynamics from experimental data.

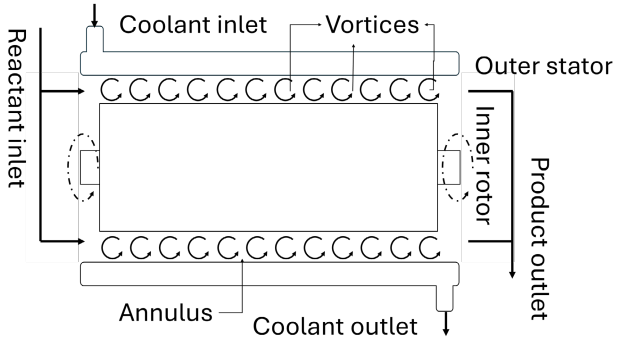

Figure 2. Axial cross section of a Taylor vortex reactor

Only this two hydrodynamics are considered in this work, yielding two options along the reactor submodel dimension.

$$c_i = c_{i0} + \frac{V}{F_{total}} \upsilon_i r; \quad (R1)$$

$$\frac{dc_i}{dV} = F_{total} \upsilon_i r; \quad (R2)$$

The reactor temperature profile expressed using the energy balance reported in Eq. (7) [15] can vary from an isothermal thermodynamic operation (Eq. D1), where the

reaction system temperature is controlled and under a constant temperature to an adiabatic thermodynamic operation (Eq. D2), where the reaction system temperature is uncontrolled and influenced by the reaction heat. These two operating modes provides the options along the thermodynamic submodel dimension.

$$dH = Q + W_s \tag{7}$$

where dH is the enthalpy change; Q is the heat transferred and W_s the shaft work impacted on the system.

$$T = constant \tag{D1}$$

$$Q = 0 \tag{D2}$$

Using these three submodel dimensions, 8 candidate models $(f_1, f_2, \dots, f_8)$ can be generated as shown in Table 1.

Table 1: The set of candidate models $\boldsymbol{f} = [f_1, f_2, \dots, f_8]$ obtained from the model generator.

	$D1$		$D2$	
	$R1$	$R2$	$R1$	$R2$
$M1$	$f_1 = (M1, R1, D1)$	$f_3 = (M1, R2, D1)$	$f_5 = (M1, R1, D2)$	$f_7 = (M1, R2, D2)$
$M2$	$f_2 = (M2, R1, D1)$	$f_4 = (M2, R2, D1)$	$f_6 = (M2, R1, D2)$	$f_8 = (M2, R2, D2)$

4.0 RESULTS AND DISCUSSION

Table 2 shows the experimental design for benzoic acid esterification where the reported kinetic models are valid.

Table 2: Benzoic acid experimental design space with three design variables and their lower and upper limits

Limits	$c_{BA}(0)$ (M)	T (K)	F_{total} $(\mu L/min)$
Lower	1.0	373.0	20.0
Upper	1.5	393.0	40.0

The impacts of three factors on the ANN classification performance are investigated: number of experiments, noise level and ANN architecture settings. In the number of experiments, five simulated experiment numbers were employed: 1 to 5, each experiment corresponding to five responses (= 4 exit chemical concentrations + 1 exit temperature). Fig. 3 shows the distribution of the 5 experiments within the experimental design space.

Two levels of constant relative noise were investigated: low (=0.01) and high (=0.1) noise level. In the ANN architecture settings, ANNfix and ANNopt were investigated. The Python optimiser package HyperOpt was employed for ANNopt. HyperOpt optimised the ANN layers and nodes along with their weights and biases during the training.

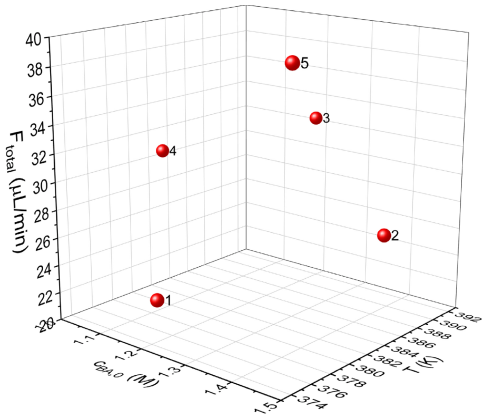

Figure 3. Distribution of 5 experiments designed using LHS in the experimental design space

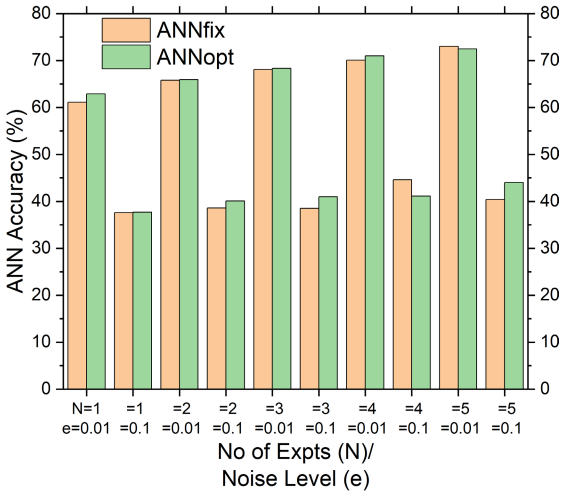

Figure 4. Comparison of the performance of the ANN network on the test dataset for the two different ANN architectures (ANNfix and ANNopt) for number of experiments between 1 and 5 and level of noise of 0.01 and 0.1.

Each of the 8 models in the model library was simulated using 1, 000 samples from the kinetic parameter space shown in Table 3. The model simulated responses in concentrations and temperature were subsequently corrupted randomly from a Gaussian distribution with a constant relative variance equalled to the level of noise.

Table 3: Benzoic acid esterification kinetic parameter space [13]

KP_1	KP_2	K_W
16.7 ± 0.02	5.93 ± 0.20	0.27 ± 0.10

The resulting in-silico data, split into training, validation and testing datasets in the ratio: 3:1:1, are fed into the ANN network. The ANN performance on the test dataset using the accuracy metric is shown in Fig. 4.

Results show that there is no significant difference between the performances of ANNfix and ANNopt in terms of global classification accuracy for the same number of experiments and level of noise. For example, when $N_{exp} = 5$ and noise level = 0.01, ANNfix achieved an accuracy of 73.0% while ANNopt achieved a slightly lower accuracy of 72.5%. At the lower number of experiments when $N_{exp} = 1$ and noise level = 0.01, ANNfix achieved an accuracy of 61.1% while ANNopt achieved only slightly a higher accuracy of 62.9%, a marginal increment not substantial enough to offset the required computational cost (86.0 seconds VS 6.7 seconds of ANNfix) and largely due to the stochastic shuffling of the datasets. Both architectures have the SoftMax activation function in the last layer required for the classification task. The input into the layer has been calculated using the trained prior network parameters and the last layer can still perform the classification, regardless of the network architectures. Further investigation confirmed that, provided the number of nodes per hidden layer in ANNfix was greater or equal to the input features, the hyperparameter optimisation employed in ANNopt did not confer a performance advantage over ANNfix. In the investigation at $N_{exp} = 20$ and 0.01 noise level, ANNfix achieved 86.3% while ANNopt achieved 86.9%. Similarly, a change in the design technique did not influence this trend. Using the full factorial design at 2 levels in the experimental design space, yielding 8 experiments from the corners in Fig. 3, ANNfix achieved 79.9% ANN classification accuracy but ANNopt performed about 2% worse at 78.1% accuracy.Different from the ANN architecture settings, other factors such as the noise level and number of experiments influence the network performance. For example, while ANNfix at a small level of noise (0.01) achieved an ANN performance of 61.1% with a single experiment, the same network architecture only achieved a performance of 37.6% at the higher noise level of 0.1. The same trend applies to ANNopt considering a single experiment, achieving 62.9% at 0.01 small noise level and 37.7% at 0.1 large noise level. By increasing the number of experiments to 2, both architectures improved in ANN performance to 65.8% and 65.9% at 0.01 noise level and to 38.6% and 40.1% at 0.1 noise level for ANNfix and ANNopt, respectively. The same trend can be observed by increasing the number of experiments further until, $N_{exp} = 5$, which has the highest ANN accuracy for both small and large noise levels in both ANN architectures. Increasing number of experiments increases the performance of the ANN while increasing noise level deteriorates the ANN performance.

The classification accuracy is illustrated graphically in Fig. 5 using the confusion matrices with two scenarios: Scenario 1 and Scenario 2. Scenario 1 corresponds to $N_{exp} = 5$ and 0.01 noise level where the achieved classification accuracy was 73.0% and Scenario 2 corresponds to $N_{exp} = 1$ and 0.1 noise level where the accuracy was 37.6 %, both considered using ANNfix architecture. The candidate models are labelled as in Table 4.

Table 4: The 8 candidate models: labels and components

Model Labels	Model components
Model 0	M1, R1, and D1
Model 1	M2, R1, and D1
Model 2	M1, R2, and D1
Model 3	M2, R2, and D1
Model 4	M1, R1, and D2
Model 5	M2, R1, and D2
Model 6	M1, R2, and D2
Model 7	M2, R2, and D2

The small noise in Scenario 1 only gives rise to classification confusion among alternative thermodynamic models (D1: isothermal and D2: adiabatic). For example, 76 out of 191 test datasets originating from Model 0 (kinetic M1, CSTR hydrodynamic R1 and isothermal thermodynamic D1) were wrongly classified as M2 (kinetic M1, CSTR hydrodynamic R1 and adiabatic thermodynamic D2). In a few instances data sets originating from a model with a CSTR hydrodynamic sub model were wrongly classified as PFR (Actual Model 2 and Predicted Model 7) or data sets originating from a model with kinetic M1 were wrongly classified as kinetic M2 (Actual Model 7 and Predicted Model 6).

In Scenario 2 with larger noise level, confusion in the ANN network classification extends beyond just one model label to multiple model labels. For example, test datasets originating from Model 0 are being wrongly classified as Model 1 (2), Model 2 (45), Model 3 (17), Model 4 (1), Model 5 (16) and Model 7 (11). Only Model 6 (kinetic M1, PFR hydrodynamic R2 and Adiabatic thermodynamic D2) was not wrongly predicted.

As a trend, the ANN performance decreases with increasing noise in the training data. At 0.01 noise variance and five simulated experiments, both ANNfix and ANNopt achieved comparable classification accuracies—73.0% and 72.5%, respectively. As noise increased to 0.1, accuracies fell below 60%, highlighting the detrimental impact of experimental uncertainty on model recognition.

Contrary to expectations [16, 17], extensive hyperparameter optimisation (ANNopt) did not improve classification performance over the fixed network (ANNfix). This suggests that data quality and diversity exert a stronger influence on model recognition accuracy than ANN complexity.

Increasing the number of simulated experiments substantially improved classification accuracy, even

under high-noise conditions. This reinforces the critical role of experimental design in ensuring model identifiability and supports the use of optimised designs in physical experimentation.

The framework provides a robust computational foundation for experimental studies in flow reactors, particularly TVRs, where mixing and thermal effects interact strongly. The ability to recognise between hydrodynamic and kinetic models rapidly can inform both reactor design and digital twin development for scale-up.

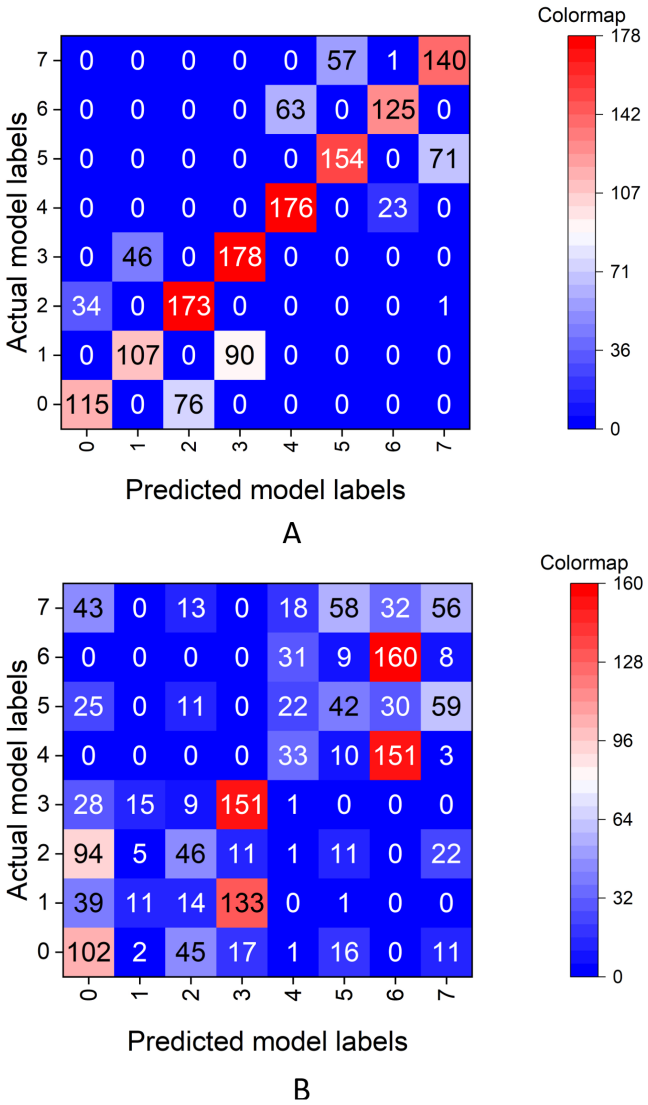

Figure 5. ANN test classification shown as confusion matrices. A) Scenario 1 ($N_{exp} = 5$, 0.01 noise level, 73.0 % accuracy); B) Scenario 2 ($N_{exp} = 1$, 0.1 noise level, 37.6 % accuracy; Model 0 (M1, R1, D1), Model 1 (M2, R1, D1), Model 2 (M1, R2, D1), Model 3 (M2, R2, D1), Model 4 (M1, R1, D2), Model 5 (M2, R1, D2), Model 6 (M1, R2, D2) and Model 6 (M2, R2, D2).

5.0 CONCLUSIONS

This study presents a hybrid digital twin framework for reactor model recognition integrating reaction kinetics, hydrodynamics, and thermodynamics. The framework combines first-principles modelling with ANN classification to achieve fast, data-driven yet physically meaningful model identification in a flow reactor system. Simulated results related to a case study of benzoic acid esterification in a Taylor vortex reactor show that ANN classification performance is highly sensitive to data noise but less dependent on network hyperparameters. Also, increasing the number of designed experiments mitigates noise effects and enhances model recognition accuracy. Hydrodynamic and thermal model inclusion improves the generality of the digital twin and its interpretability.

This work highlights the importance of combining physics-based and data-driven approaches in reactor model identification and provides a foundation for hybrid digital twin development in chemical and pharmaceutical manufacturing. Future work will therefore focus on the extension of the model library and the integration with the physical system.

DIGITAL SUPPLEMENTARY MATERIAL

Source Code: The code used in this work is available in GitHub at https://github.com/emmanagun/A-General-Artificial-Neural-Networks-Framework-for-Model-Recognition-in-Chemical-Reactor-Systems

ACKNOWLEDGEMENTS

This research was funded by EPSRC (grant number: EP/X024016/1).

AUTHOR IDENTIFIERS

Author ORCIDs:
Agunloye E: 0000-0002-1076-8385
Gavriilidis A: 0000-0003-3508-5043
Galvanin F: 0000-0002-3296-1581

REFERENCES

1. Galvanin F, Hartman RL, Kulkarni AA, Nieves-Remacha MJ. Introduction to the themed collection on digitalization in reaction engineering. React. Chem. Eng. 7:792-794 (2022). https://doi.org/10.1039/d2re90011d
2. Peterson L, Gosea IV, Benner P, Sundmacher K. Digital twins in process engineering: an overview on computational and numerical methods. Computers & Chemical Engineering

193:108917 (2025). https://doi.org/10.1016/j.compchemeng.2024.108917
3. Kasilingam S, Yang R, Singh SK, Farahani MA, Rai R, Wuest T. Physics-based and data-driven hybrid modeling in manufacturing: a review. Production & Manufacturing Research 12: (2024). https://doi.org/10.1080/21693277.2024.2305358
4. Destro F, Barolo M. A review on the modernization of pharmaceutical development and manufacturing – trends, perspectives, and the role of mathematical modeling. International Journal of Pharmaceutics 620:121715 (2022). https://doi.org/10.1016/j.ijpharm.2022.121715
5. Chen Y, Ierapetritou M. A framework of hybrid model development with identification of plant?model mismatch. AIChE Journal 66: (2020). https://doi.org/10.1002/aic.16996
6. Narayanan H, Luna M, Sokolov M, Arosio P, Butté A, Morbidelli M. Hybrid models based on machine learning and an increasing degree of process knowledge: application to capture chromatographic step. Ind. Eng. Chem. Res. 60:10466-10478 (2021). https://doi.org/10.1021/acs.iecr.1c01317
7. Geremia M, Marella T, Ardalani E, Beyramysoltan S, Chattoraj S, Facco P, Barolo M, Bezzo F. On the impact of mechanistic model quality and data availability in hybrid model development. Computers & Chemical Engineering 206:109536 (2026). https://doi.org/10.1016/j.compchemeng.2025.109536
8. Bird RB, Stewart WE and Lightfoot EN, Transport Phenomena (Second ed.). *John Wiley & Sons* (2001)
9. Quaglio M, Roberts L, Bin Jaapar MS, Fraga ES, Dua V, Galvanin F. An artificial neural network approach to recognise kinetic models from experimental data. Computers & Chemical Engineering 135:106759 (2020). https://doi.org/10.1016/j.compchemeng.2020.106759
10. Sangoi E, Quaglio M, Bezzo F, Galvanin F. An optimal experimental design framework for fast kinetic model identification based on artificial neural networks. Computers & Chemical Engineering 187:108752 (2024). https://doi.org/10.1016/j.compchemeng.2024.108752
11. Agunloye E, Gavriilidis A, Galvanin F. Hybrid modelling framework for reactor model discovery using artificial neural networks classifiers. SUSTENS 2025 :11 (2025). https://doi.org/10.3390/proceedings2025121011
12. Heaton J. Ian goodfellow, yoshua bengio, and aaron courville: deep learning. Genet Program Evolvable Mach 19:305-307 (2017). https://doi.org/10.1007/s10710-017-9314-z
13. Waldron C, Pankajakshan A, Quaglio M, Cao E, Galvanin F, Gavriilidis A. Closed-loop model-based design of experiments for kinetic model discrimination and parameter estimation: benzoic acid esterification on a heterogeneous catalyst. Ind. Eng. Chem. Res. 58:22165-22177 (2019). https://doi.org/10.1021/acs.iecr.9b04089
14. Fogler HS, Elements of Chemical Reaction Engineering, Prentice -Hall, Upper Saddle (2004) New Jersey
15. Sandler SI, Chemical, Biochemical, and Engineering Thermodynamics, fourth ed., John Wiley and Sons (2006) New Jersey.
16. Du X, Xu H, Zhu F. Understanding the effect of hyperparameter optimization on machine learning models for structure design problems. Computer-Aided Design 135:103013 (2021). https://doi.org/10.1016/j.cad.2021.103013
17. Sun L. Automated neural network architecture design and hyperparameter adjustment integrating distribution-based optimization strategy. ACE 147:181-186 (2025). https://doi.org/10.54254/2755-2721/2025.22721